**Biogeosciences
Discussions**

Biological productivity in the Mauritanian upwelling estimated with a triple gas approach

T. Steinhoff[1], H. W. Bange[1], A. Kock[1], D. W. R. Wallace[2], and A. Körtzinger[1]

[1]GEOMAR | Hemholtz Centre for Ocean Research, Kiel, Germany
[2]Department of Oceanography, Dalhousie University, Halifax, Nova Scotia, Canada

Correspondence to: T. Steinhoff (tsteinhoff@geomar.de)

Abstract

Due to their high biological productivity coastal upwelling regions are important for biogeochemical cycles in the ocean and for fisheries. Upwelled water is not only enriched in nutrients but also supersaturated with respect to atmospheric CO_2 and N_2O and undersaturated for O_2. We present a novel approach to estimate carbon based net community production (NCP) using surface ocean data for CO_2, O_2 and N_2O from three cruises to the Mauritanian upwelling region (Northwest Africa) that were conducted in different seasons. Through combination of the saturation patterns of CO_2, O_2 and N_2O effects of air–sea gas exchange and NCP could be separated. NCP values ranges from $0.6 \pm 0.1\,\mathrm{g\,C\,m^{-2}\,d^{-1}}$ during times of weak upwelling to $1.6 \pm 0.4\,\mathrm{g\,C\,m^{-2}\,d^{-1}}$ during strong upwelling. The estimated NCP values show a strong relationship with a wind derived upwelling index, which was used to estimate annual NCP.

1 Introduction

Eastern Boundary Upwelling Ecosystems (EBUE) are amongst the most productive regions of the world ocean with corresponding importance both for fisheries and for the cycling of carbon in the ocean (Pauly and Christensen, 1995). Approximately 11 % of global primary production (PP) is generated in EBUE although they account for only about 1 % of the ocean's surface area (Chavez and Toggweiler, 1995). The upwelling along the west coasts of continents is driven by Trade Winds acting in concert with the Coriolis force, and injects nutrients from below the surface into the ocean's euphotic zone triggering high PP. The Canary Current Ecosystem is one of four major EBUE and exhibits the strongest spatial and seasonal variability of PP, with more or less constant upwelling in its northern section (19° N–33° N) and pronounced seasonality south of 19° N (Carr and Kearns, 2003). The studied region off the Mauritanian coast between 17° N and 21° N is known as the transition zone between the constant and seasonal upwelling regimes (Wooster et al., 1976).

PP in upwelling areas has been estimated variously from modeling studies (Lachkar and Gruber, 2011), using remotely sensed data as proxies (Behrenfeld et al., 2005; Messié et al., 2009), and from incubation measurements (Dugdale and Goering, 1967). The latter provide instantaneous local productivity estimates which suffer from potential artifacts due to incubation effects whereas remotely sensed estimates cover larger areas but have other sources of bias, e.g. atmospheric correction for dust (Chavez and Messié, 2009). Minas et al. (1986) derived production estimates for the Mauritanian upwelling by direct measurements of nutrients and their subsequent decrease in combination with the heat flux of the surface water. Their method is somewhat similar to our approach and resulted in an estimate of net community production (NCP, which is gross primary production minus respiration). However, there is evidence that nutrient uptake is not an ideal measure for productivity as the elemental ratio (C/N) can vary significantly during production (Sambrotto et al., 1993; Thomas et al., 1999) due to changing communities and available nutrients (Koeve, 2004; Körtzinger et al., 2001a).

Here we present a novel approach for carbon based estimation of NCP by using direct surface measurements of the partial pressure of CO_2 (pCO_2), O_2 and N_2O. The approach is applied to data collected during three cruises to the Mauritanian upwelling region (Fig. 1) during different years and different seasons: R/V Poseidon Cruise 320-1 (P320-1, March 2005, intense upwelling), R/V Meteor Cruise 68-3 (M68-3, July 2006, weak upwelling) and R/V Poseidon Cruise 399-2 (P399-2, June 2010, transition from intense to weak upwelling).

2 Data and methods

2.1 Measurements

On all cruises, seawater was supplied to the pCO_2 and N_2O instruments by a submersible impeller pump, which was installed in the ships' moon pool at approximately 5 m depth. For measurement of sea surface temperature (SST) and sea surface salinity

(SSS) a submersible CTD (Eco-Probe, ME-Grisard, Germany) was installed next to the submersible pump. Atmospheric pressure and wind speed data were taken from the ships' weather stations. All temperature probes (in-situ and in the equilibrator) were calibrated against international standards.

The pCO_2 system that was used during P320-1 and M68-3 is described in detail in Körtzinger et al. (1996). Seawater was pumped through an equilibrator (2-stage equilibrator with laminar flow and bubble stage), subsequently dried and measured via a LICOR NDIR gas analyzer. During P399-2 a commercially available pCO_2 system was used (General Oceanics, Miami, USA). The measurement principle is the same but the equilibrator is a shower head type (Pierrot et al., 2009). For the calibration of the NDIR analyzer standard gases were used: The analysis cycle involved a calibration cycle every three hours during which a suite of three standard gases (nominal concentrations ranging between 250 and 670 ppm CO_2 in natural air) was measured. These working standard gases were calibrated against NOAA primary standards with similar concentration ranges using a LI-COR NDIR analyzer (model 6262). The achieved accuracy was 0.13 ppm. Once a day a CO_2 free gas and the highest standard were used to adjust the NDIR analyzer for small instrument drift. A detailed description of the data reduction is given in Steinhoff (2010). However, the overall accuracy of pCO_2 measurements is estimated to be < 3 µatm.

Nitrous oxide was determined via a gas chromatograph (GC) with an electron capture detector. A detailed description of the method is given in (Walter et al., 2004). Seawater N_2O was measured using a shower head equilibrator, and with the same GC as atmospheric N_2O. The accuracy of the underway measurements was determined to be $\pm 1\%$.

For the underway measurements of O_2 an oxygen optode (Aanderaa, Bergen, Norway) was used. The optode was placed in an insulated box, that was flushed with the seawater supplied by the pump with a flow rate of approximately $10\,l\,min^{-1}$. The optode data were calibrated against discrete samples taken from the CTD casts (upper 4–8 m Niskins). The discrete samples were measured by standard Winkler titration.

The overall accuracy of the optode measurements was estimated to be $\pm 3\,\mu\mathrm{mol\,l^{-1}}$ for P320-1 and $\pm 5\,\mu\mathrm{mol\,l^{-1}}$ for M68-3 and P399-2.

In addition to the underway measurements discrete samples were taken for dissolved inorganic carbon (DIC), alkalinity (AT) and nutrients, both from the underway installation and from the profiling CTD (upper 4–8 m niskins). DIC and AT samples were measured on board following the recommendations of Dickson et al. (2007). Certified water samples were used to estimate accuracy ($\pm 2.2\,\mu\mathrm{mol\,kg^{-1}}$ and $\pm 4.7\,\mu\mathrm{mol\,kg^{-1}}$ for DIC and AT, respectively).

Nitrate samples were also measured on board with a continuous-flow-autoanalyzer following the method of Hansen and Koroleff (1999). The overall accuracy for nitrate analysis was 1 %. The precision was determined by duplicate measurements and resulted in $0.12\,\mu\mathrm{mol\,l^{-1}}$.

Table 1 shows the measured data (underway and discrete) and their typical measurement frequency.

2.2 Ancilliary data

For the present study we also employed additional data sources for parameters such as mixed layer depth (MLD), upwelling index (UI) and atmospheric CO_2 concentration. For MLD estimates we used the model output of the Mercator project (http://www.mercator-ocean.fr) since it has been shown to be in good agreement with MLD estimates derived with accepted standard criteria applied on profile data (Steinhoff et al., 2010). We compared the model derived MLD with MLD estimated from measured profile data and they were in good agreement. The model output yield one MLD estimate based on a temperature criterion and one based on a density criterion. We used the mean MLD value of these for each grid cell ($1/6° \times 1/6°$).

The Pacific Fisheries Environmental Laboratory (PFEL) provides 6-hourly upwelling indices on a $1° \times 1°$ grid for coastal regions, which are derived from pressure field data. We used the data at 18.5° N, 16.5° W. Due to the high fluctuations of the 6-hourly data

we used an asymmetric running mean of 14 days (13 days back) to calculate daily UI. To allocate an UI to the NCP measurement for each cruise we chose the mean value for the whole time of the cruise.

For the calculation of atmospheric $p\mathrm{CO_2}$ we used $x\mathrm{CO_2}$ data from GLOBALVIEW (GLOBALVIEW-CO2, 2011). They are in good agreement with our own measurements but do not contain short term fluctuations associated with air mass trajectories that do not significantly influence seawater $p\mathrm{CO_2}$ because of the long gas exchange time scale. We choose $x\mathrm{CO_2}$ data from two stations and linearly interpolated between them ($x\mathrm{CO_2} = f$ (Latitude)): Azores (AZR: 38.77° N, −27.38° W) and Barbados (RPB: 13.17° N, 59.43° W).

3 Calculation of NCP

Subsurface waters in upwelling regions are typically not only enriched in nutrients but also in dissolved inorganic carbon (DIC; by respiration) and N_2O (by nitrification) and low in O_2 (by respiration). Upwelling of these waters results in strong near-surface supersaturation and subsequent outgassing of CO_2 and N_2O, together with undersaturation and ingassing of O_2.

Figure 2 shows measurements of $p\mathrm{CO_2}$, N_2O and O_2 sampled along a transect from the open ocean to the coast during a period of intense upwelling (cruise P320-1). High supersaturations of CO_2 and N_2O and undersaturation of O_2 were observed along a narrow band influenced by upwelling near the coast. Concentrations and supersaturations (undersaturation) decreased (increased) with distance offshore, reaching concentrations that were in equilibrium with the atmosphere ca. 200 km offshore.

We assume that nitrification is a negligible source of additional N_2O for the surface layer due to its inhibition by light (Horrigan et al., 1981). Nitrifying organisms that were observed in the upper 100 m of an upwelling filament in this region are therefore considered to supply only a minor contribution to the N_2O budget of surface waters (Rees et al., 2011). Also turbulent transport into the mixed layer from below can be neglected

(Schafstall et al., 2010). The study of Kock et al. (2012) that took place in the same study region also concluded that N_2O production in the upwelled water off Mauritania is unlikely. Thus the offshore decrease of N_2O concentrations is assumed to be driven only by ASE. In contrast, CO_2 changes in the surface water are mediated by both ASE and concurrent NCP, the separation of which is not straight forward (Service et al., 1998).

Our novel triple gas approach exploits the initial, strongly non-equilibrium dissolved gas concentrations in newly-upwelled waters and the dominant role of ASE for the subsequent evolution of N_2O concentrations in order to separate the effects of NCP and ASE on the evolution of CO_2 and O_2 concentrations.

In effect, we use N_2O as a biogeochemically "inert" tracer of ASE which provides a measure of "time since upwelling" for surface waters in the region. This is done by calculating the hypothetical temporal evolution of surface layer N_2O concentrations from the initial observed supersaturation towards equilibrium levels for realistic parameterizations of ASE. The N_2O-derived "time stamps" can then be assigned to the co-located, contemporary CO_2 and O_2 measurements.

For the following calculation of NCP the measured pCO_2 values need to be converted into DIC values. This was done using CO2sys (van Heuven et al., 2009) and as input parameters pCO_2 and AT. Because of its low variability, a mean value of AT ($2362\,\mu mol\,kg^{-1}$, cf. Table 2) was chosen for the whole dataset. A theoretical equilibrium DIC (DIC_{equ}) was calculated analogously by replacing seawater pCO_2 with atmospheric pCO_2 ($pCO_{2,atm}$).

Transfer velocities k were calculated for N_2O and CO_2 using the parameterization of Wanninkhof (1992) and Tsai and Liu (2003).

We used the N_2O data to estimate the time τ that has passed since a water parcel had upwelled, i.e. highest observed seawater N_2O (N_2O_{sw}) concentrations denote freshly upwelled water and thus the origin of the time axis ($\tau = 0$).

Furthermore N_2O_{sw} serves as a central variable for the NCP calculations and the relationships between N_2O_{sw} and various variables that were needed for our calculation

4859

were determined: N_2O_{equ}, DIC_{equ}, AT, SSS, SST, k_{N_2O}, k_{CO_2} and MLD (Table 2). Linear relationships were used where suitable otherwise the mean value was used.

Relating N_2O_{equ} to N_2O_{sw} is a sort of circular argument, when calculating ASE. But all these relationships do not necessarily have biogeochemical meaning and were only used to provide N_2O_{sw} values with matching values of other parameters.

Figure 3 illustrates the calculations that were performed to derive NCP for every cruise. The shown data are from the cruise P320-1:

(A) Iterative calculation of N_2O air–sea equilibration time scale

The dataset was searched for highest N_2O_{sw} concentration (red marker) and it was confirmed that the location of this point was indeed in the core upwelling region. Using the average mixed layer depth (MLD) the concentration was converted into a mixed layer inventory:

$$N_2O_{inv} = N_2O_{sw} \times MLD \tag{1}$$

Next, the daily ASE fluxes for N_2O were calculated based on ΔN_2O:

$$F_{N_2O} = k_{N_2O} \times \Delta N_2O = k_{N_2O} \times (N_2O_{sw} - N_2O_{equ}) \tag{2}$$

where k_{N_2O} is the transfer coefficient for N_2O at SST (Table 2). Matching values for SST and N_2O_{equ} were calculated from N_2O_{sw} as described above. Subtracting the daily loss of N_2O due to ASE (F_{N_2O}) from the inventory resulted in a new inventory which was converted back into N_2O_{sw} concentration using MLD. These daily inventory/flux cycle calculations were performed until the time τ_{max} when ΔN_2O was less than $0.1\,nmol\,l^{-1}$, i.e. N_2O air–sea equilibrium was practically reached. The resulting temporal evolution of the N_2O_{sw} concentrations is shown in Fig. 3a. A function was fitted to these N_2O data and a value for τ was assigned to each measured N_2O_{sw} value.

(B) Application of time stamp to DIC data

4860

With the results from (A) τ was assigned to each DIC_{sw} value where both, DIC_{sw} and N_2O_{sw}, measurements were available. An exponential function was then fitted to the data (Fig. 3b). With this function a value of τ was assigned to every DIC_{sw} value even when no concurrent N_2O_{sw} value was available.

(C) Iterative calculation to separate F_{ASE} and F_{bio} for CO_2

With the results from (A) and (B), the CO_2 ASE flux per day was calculated. Starting with DIC_{sw} values at time step 1 and 2 (i.e., τ_1 and τ_2) these values were converted into inventories I ($I(\tau_1)$ and $I(\tau_2)$). Matching values for DIC_{equ}, SSS and SST were calculated from N_2O_{sw} at τ_1 (Table 2) and the CO_2 ASE flux F_{ASE} was calculated using $F_{ASE} = k_{CO_2} \times k_0 \times \Delta pCO_2$, where k_{CO_2} is the transfer coefficient and k_0 the solubility of CO_2. A new inventory was calculated which was influenced only by ASE:

$$I_{ASE}(\tau_2) = I(\tau_1) - F_{ASE} \tag{3}$$

The difference between the calculated $I_{ASE}(\tau_2)$ and the observed inventory $I(\tau_2)$ is assumed to represent the CO_2 that was consumed by biology during the first time step:

$$F_{bio} = I_{ASE}(\tau_2) - I(\tau_2) \tag{4}$$

The calculation was then repeated for every single time step – always starting with the observed DIC for a given time τ_i, calculating the ASE on the basis of the corresponding pCO_2 level, and comparing the resulting hypothetical DIC with the observed DIC at time τ_{i+1} – until τ_{max} was reached. The resulting daily biological flux, F_{bio}, is shown in Fig. 3c.

(D) Calculation of biological CO_2 drawdown (DIC_{bio})

MLD was used to calculate the amount of biological CO_2 drawdown:

$$DIC_{bio} = \frac{F_{bio}}{MLD} \tag{5}$$

When the change of DIC_{bio} per day was less than $2\,\mu mol\,l^{-1}$, this day was defined as the end of the upwelling mediated productive period (τ_{bio}). The overall amount of CO_2 that was consumed by biology is the sum of all daily estimates of DIC_{bio} until τ_{bio}:

$$DIC_{bio}^{tot} = \sum_{\tau=1}^{\tau_{bio}} DIC_{bio}(\tau) \tag{6}$$

NCP was calculated as follows:

$$NCP = DIC_{bio}^{tot} \times MLD \times \frac{1}{\tau_{bio}} \times 0.012 \tag{7}$$

where NCP is in $g\,C\,m^{-2}\,d^{-1}$, DIC_{bio}^{tot} in $mmol\,m^{-3}$, MLD in m and τ_{bio} in days. The factor 0.012 converts to gravimetric units of carbon.

This calculation was performed for all three cruises. The resulting NCP estimates and the corresponding duration of the productivity phase are given in Table 3.

4 Results and discussion

Clearly the calculation, and hence the NCP estimate, depends critically on the choice of wind speed dependent parameterization for the gas transfer coefficient k (e.g., Wanninkhof (1992) and several recent ones). Furthermore there is evidence that in highly productive regions surfactants significantly reduce the gas transfer velocity (Kock et al., 2012; Schmidt and Schneider, 2011; Tsai and Liu, 2003).

However, the budget of O_2, which is also controlled by ASE and NCP, provides an independent constraint on the choice of transfer coefficient. Given that there is a tight stoichiometric link of NCP-driven changes in DIC and O_2 (i.e., photosynthetic quotient), the choice of parameterization for the gas transfer coefficient can be constrained by the requirement that the resulting NCP estimates based on DIC and O_2 budgets agree

within error bars. We found that use of the common parameterization of Wanninkhof (1992) resulted in unrealistic photosynthetic quotients that could not be explained by error propagation in the calculation scheme, thus pointing the inapplicability of the common parameterizations in this particular setting. Note, that this calculation was only performed for the cruise P320-1, because the precision of the O_2 measurements was not adequate for calculation of O_2 fluxes on the other cruises. Consequently we used a parameterization that accounts for the effect of surfactants (Tsai and Liu, 2003) to calculate N_2O, CO_2 and O_2 fluxes for the cruises P320-1 and P399-2, which took place during periods of increased productivity. Cruise M68-3, on the other hand, took place during a period of only marginal upwelling (and hence lower productivity) and therefore k was calculated using the relationship of Wanninkhof (1992). When using the parameterization of Tsai and Liu (2003), a O_2/CO_2 ratio of NCP of -1.27 was found over the first 12 days of production during which more than 90 % of NCP had been accomplished. Using the parameterization of Wanninkhof (1992) resulted in a O_2/CO_2 ratio of -0.75. The value of -1.27 is slightly lower than the value published by Laws (1991) (-1.4 to -1.5), but compares well with the original value of -1.30 by Redfield et al. (1963) and the findings of Wallace et al. (1995) (-1.27 ± 0.14) and Körtzinger et al. (2001b) (-1.34).

We also used discrete surface nitrate measurements from these cruises to calculate the C/N ratio of NCP. For the first 12 days of production the C/N value was calculated as $5.9 \pm 0.05(1\sigma)$ which is somewhat lower than the canonical Redfield ratio of 6.6 (Redfield et al., 1963), a situation that might hint at nitrogen overconsumption which has been documented for nutrient replete conditions (Körtzinger et al., 2001a), but certainly is within the error bars of the NCP estimate.

A connection between productivity and upwelling intensity has been reported by several studies (Dugdale and Goering, 1967, and references herein). Figure 4a shows the seasonal and interannual variability of the Mauritanian upwelling intensity (expressed by the UI) for the years 2005–2010. The maximum upwelling intensity is always found during the late boreal winter and can vary interannually by about ±20 %. Figure 4a

4863

also shows our NCP estimates for the period covered by our field studies. High NCP is observed at or near the maximum of upwelling in 2005 and lowest NCP during the late summer in 2006 when upwelling intensity is at its minimum. The cruise in 2010 took place during the transition phase from intense to weak upwelling and intermediate NCP was observed. Minas et al. (1986) estimated NCP to be $2.3\,\mathrm{g\,C\,m^{-2}\,d^{-1}}$ for a transect north of our study region ($21°\,N$). Their value is significantly higher than our estimates even though the upwelling intensity during their study was not (UI = 260, data not shown). This might be due to several reasons including: (i) their different estimation approach for NCP (i.e., using nutrients for productivity estimates), (ii) the different location and zonal extent of the data set, (iii) the fact that their study took place in the part of the upwelling where more constant upwelling is observed throughout the year (different upwelling systems respond differently on the upwelling intensities (Lachkar and Gruber, 2012)).

Our results show a clear linear relationship between the estimated NCP and the upwelling index (Fig. 4b). With only three data points, the exact slope of the relationship is currently not well constrained. The relationship does, however, hint at potential predictability of NCP from wind-driven upwelling intensity, which would have major implication for future predictions. It was used to calculate annual NCP budgets based on the upwelling index for the period 2005–2010. The annual NCP budget varies between 324 and $401\,\mathrm{g\,C\,m^{-2}\,yr^{-1}}$. For comparison, a mean value of $539\,\mathrm{g\,C\,m^{-2}\,yr^{-1}}$ for "potential new production" was reported in the area between $12°\,N$ and $22°\,N$ and for the years 1999–2008 (Messié et al., 2009).

5 Conclusions

Here we presented a novel method to estimate NCP in a coastal upwelling system by direct measurements of three gases which are affected by ASE and/or by NCP. As changes in CO_2 concentration were observed directly this approach is independent from variable C/N ratios. CO_2 and N_2O data were used to separate ASE and NCP, but

4864

a third variable (in our case O_2) is needed to constrain ASE. Furthermore, the results support the findings of other studies that in highly productive areas of the ocean surfactants may strongly attenuate ASE. The dependence of NCP on upwelling intensity (which itself depends on wind fields) make the EBUE sensible to global warming, i.e. intensification of upwelling with increased temperatures (McGregor et al., 2007).

References

Behrenfeld, M. J., Boss, E., Siegel, D. A., and Shea, D. M.: Carbon-based ocean productivity and phytoplankton physiology from space, Global Biogeochem. Cy., 19, GB1006, doi:10.1029/2004GB002299, 2005.

Carr, M.-E. and Kearns, E. J.: Production regimes in four eastern boundary current systems, Deep-Sea Res. Pt. II, 50, 3199–3221, doi:10.1016/j.dsr2.2003.07.015, 2003.

Chavez, F. P. and Toggweiler, J. R.: Physical estimates of global new production: the upwelling contribution, in: Upwelling in the Ocean: Modern Processes and Ancient Records, edited by: Summerhayes, C. P., Emeis, K. C., Angel, M. V., Smith, R. L., and Zeitzschel, B., Wiley, Chichester, 313–320, 1995.

Chavez, F. P. and Messié, M.: A comparison of eastern boundary upwelling ecosystems, Progr. Oceanogr., 83, 80–96, 2009.

Dickson, A. G., Sabine, C. L., and Christian, J. R. (Eds.): Guide to Best Practices for Ocean CO_2 Measurements, PICES Special Publication 3, Sidney, Canada, 2007.

Dugdale, R. C. and Goering, J. J.: Uptake of new and regenerated forms of nitrogen in primary productivity, Limnol. Oceanogr., 12(2), 196–206, 1967.

GLOBALVIEW-CO_2: Cooperative Atmospheric Data Integration Project – Carbon Dioxide, CD-ROM, NOAA ESRL, Boulder, Colorado, also available on Internet via anonymous FTP to ftp.cmdl.noaa.gov, last access: February 2012, Path: ccg/co2/GLOBALVIEW, 2011.

Hansen, H. P. and Koroleff, F.: Determination of nutrients, in: Methods of Seawater Analysis, edited by: Grasshoff, K., Kremling, K., and Erhardt, M., Verlag Chemie, Weinheim, 159–228, 1999.

Horrigan, S. G., Carlucci, A. F., and Williams, P. M.: Light inhibition of nitrification in sea-surface films, J. Mar. Res., 39(3), 557–565, 1981.

Kock, A., Schafstall, J., Dengler, M., Brandt, P., and Bange, H. W.: Sea-to-air and diapycnal nitrous oxide fluxes in the eastern tropical North Atlantic Ocean, Biogeosciences, 9, 957–964, doi:10.5194/bg-9-957-2012, 2012.

Koeve, W.: Spring bloom carbon to nitrogen ratio of net community production in the temperate N. Atlantic, Deep-Sea Res. Pt. I, 51(11), 1579–1600, doi:10.1016/j.dsr.2004.07.002, 2004.

Körtzinger, A., Thomas, H., Schneider, B., Gronau, N., Mintrop, L., and Duinker, J. C.: At-sea intercomparison of two newly designed underway pCO$_2$ systems – encouraging results, Mar. Chem., 52, 133–145, 1996.

Körtzinger, A., Koeve, W., Kähler, P., and Mintrop, L.: C:N ratios in the mixed layer during the productive season in the Northeast Atlantic Ocean, Deep-Sea Res. Pt. I, 48, 2001a.

Körtzinger, A., Hedges, J. I., and Quay, P. D.: Redfield ratios revisited: removing biasing effect of anthropogenic CO_2, Limnol. Oceanogr., 46(4), 964–970, 2001b.

Lachkar, Z. and Gruber, N.: What controls biological production in coastal upwelling systems? Insights from a comparative modeling study, Biogeosciences, 8, 2961–2976, doi:10.5194/bg-8-2961-2011, 2011.

Lachkar, Z. and Gruber, N.: A comparative study of biological production in eastern boundary upwelling systems using an artificial neural network, Biogeosciences, 9, 293–308, doi:10.5194/bg-9-293-2012, 2012.

Laws, E. A.: Photosynthetic quotients, new production and net community in the open ocean, Deep-Sea Res. Pt. A, 38(1), 143–167, 1991.

McGregor, H. V., Dima, M., Fischer, H. W., and Mulitza, S.: Rapid 20th-century increase in coastal upwelling off Northwest Africa., Science, 315(5812), 637–639, doi:10.1126/science.1134839, 2007.

Messié, M., Ledesma, J., Kolber, D. D., Michisaki, R. P., Foley, D. G., and Chavez, F. P.: Potential new production estimates in four eastern boundary upwelling ecosystems, Progr. Oceanogr., 83, 151–158, 2009.

Minas, H. J., Minas, M., and Packard, T. T.: Productivity in upwelling areas deduced from hydrographic and chemical fields, Limnol. Oceanogr., 31(6), 1182–1206, 1986.

Pauly, D. and Christensen, V.: Primary production required to sustain global fisheries, Nature, 374, 255–257, doi:10.1038/374255a0, 1995.

Pierrot, D., Neill, C., and Sullivan, K.: Recommendations for autonomous underway pCO$_2$ measuring systems and data-reduction routines, Deep-Sea Res. Pt. II, 56(8–10), 512–522, doi:10.1016/j.dsr2.2008.12.005, 2009.

Redfield, A. C., Ketchum, B. H., and Richards, F. A.: The influence of organisms on the composition of seawater, in: The Sea, Vol. 2, edited by: Hill, M. N., Interscience, New York, 26–77, 1963.

Rees, A. P., Brown, I. J., Clark, D. R., and Torres, R.: The Lagrangian progression of nitrous oxide within filaments formed in the Mauritanian upwelling, Geophys. Res. Lett., 38(21), 1–6, doi:10.1029/2011GL049322, 2011.

Sambrotto, R. N., Savidge, G., Robinson, C., Boyd, P., Takahashi, T., Karl, D. M., Langdon, C., Chipman, D., Marra, J., and Codispoti, L.: Elevated consumption of carbon relative to nitrogen in the surface ocean, Nature, 363, 248–250, 1993.

Schafstall, J., Dengler, M., Brandt, P., and Bange, H.: Tidal-induced mixing and diapycnal nutrient fluxes in the Mauritanian upwelling region, J. Geophys. Res., 115(C10), 1–19, doi:10.1029/2009JC005940, 2010.

Schmidt, R. and Schneider, B.: The effect of surface films on the air–sea gas exchange in the Baltic Sea, Mar. Chem., 126(1–4), 56–62, doi:10.1016/j.marchem.2011.03.007, 2011.

Service, S. K., Rice, J. A., and Chavez, F. P.: Relationship between physical and biological variables during the upwelling period in Monterey Bay, CA, Deep-Sea Res. Pt. II, 45, 1669–1685, doi:10.1016/S0967-0645(98)80012-X, 1998.

Steinhoff, T.: Carbon and nutrient fluxes in the North Atlantic Ocean, University of Kiel, 162 pp., available at: http://eldiss.uni-kiel.de/macau/receive/dissertation_diss_00005704, last access: February 2012, 2010.

Steinhoff, T., Friedrich, T., Hartman, S. E., Oschlies, A., Wallace, D. W. R., and Körtzinger, A.: Estimating mixed layer nitrate in the North Atlantic Ocean, Biogeosciences, 7, 795–807, doi:10.5194/bg-7-795-2010, 2010.

Thomas, H., Ittekot, V., Osterroht, C., and Arnold, E.: Preferential recycling of nutrients — the ocean's way to increase new production and to pass nutrient limitation?, Limnol. Oceanogr., 44(8), 1999–2004, 1999.

Tsai, W. and Liu, K.: An assessment of the effect of sea surface surfactant on global atmosphere-ocean CO$_2$ flux, J. Geophys. Res., 108(C4), 1–16, doi:10.1029/2000JC000740, 2003.

van Heuven, S., Pierrot, D., Lewis, E., and Wallace, D. W. R.: MATLAB Program Developed for CO$_2$ System Calculations, ORNL/CDIAC-105b, ORNL/CDIAC, Oak Ridge, Tennessee, 2009.

Wallace, D. W. R., Minnett, P. J., and Hopkins, T. S.: Nutrients, oxygen, and inferred new production in the Northeast Water Polynya, 1992, J. Geophys. Res., 100(C3), 4323–4340, 1995.

Walter, S., Bange, H. W., and Wallace, D. W. R.: Nitrous oxide in the surface layer of the tropical North Atlantic Ocean along a west to east transect, Geophys. Res. Lett., 31(23), 4–7, doi:10.1029/2004GL019937, 2004.

Wanninkhof, R.: Relationship between wind speed and gas exchange over the ocean, J. Geophys. Res., 97(C5), 7373–7382, 1992.

Wooster, W. S., Bakun, A., and McLain, D. R.: The seasonal upwelling cycle along the eastern boundary of the North Atlantic, J. Mar. Res., 34(2), 131–141, 1976.

Table 1. Measured data that were used for this study and their typical sampling frequency.

Parameter	Discrete	Underway	Sampling interval
Seawater pCO_2		×	1 min
Seawater N_2O		×	40 min
Equilibrium N_2O		×	40 min
Dissolved oxygen		×	1 min
SST		×	1 min
SSS		×	1 min
Wind speed		×	1 min
Atmospheric pressure		×	1 min
AT	×		
Nitrate	×		

Table 2. Regression parameters and root mean square errors (RMSE) for parameters that were estimated from N_2O_{sw} concentrations. Note that there is no biogeochemical reason for the fits and they were exclusively used to match N_2O_{sw} values with corresponding values of regressed variables. The lower part shows mean values of the parameters that couldn't be parameterized and had to be taken as averages. The values in parentheses are the standard deviations.

	P320-1		M68-3		P399-2	
	r^2	RMSE	r^2	RMSE	r^2	RMSE
Regression parameters						
N_2O_{equ} (nmol l^{-1})	0.91	0.09	0.81	0.11	0.96	0.26
DIC_{equ} (µmol kg^{-1})	0.87	3.6	0.76	5.1	0.27	14.06
SSS	0.52	0.01	0.76	0.03	0.54	0.04
SST (°C)	0.91	0.37	0.84	0.53	0.7	1.15
Mean values (±1σ)						
MLD (m)	25(±10)		13(±5)		18(±6)	
AT (µmol kg^{-1})	2362(±11)		2362(±11)		2362(±11)	
k_{N_2O} (Wanninkhof, 1992) (cm h^{-1})	21.7(±5.8)		7.7(±8.0)		21.1(±8.1)	
k_{N_2O} (Tsai and Liu, 2003) (cm h^{-1})	5.4(±1.2)		1.5(±2.1)		5.2(±1.7)	
k_{CO_2} (Wanninkhof, 1992) (cm h^{-1})	22.2(±5.9)		7.3(±8.5)		21.6(±8.3)	
k_{CO_2} (Tsai and Liu, 2003) (cm h^{-1})	5.5(±1.2)		1.5(±2.2)		5.3(±1.8)	
k_{O_2} (Wanninkhof, 1992) (cm h^{-1})	23.6(±6.3)		7.7(±9.0)		22.8(±8.7)	
k_{O_2} (Tsai and Liu, 2003) (cm h^{-1})	6.1(±1.3)		1.6(±2.3)		5.6(±1.9)	

Table 3. Upwelling index, NCP and duration of productivity phase as estimated in this study.

Cruise	Mean upwelling index	NCP $(\mathrm{g\,C\,m^{-2}\,d^{-1}})$	Duration of productivity phase (d)
P320-1	345	1.6(±0.4)	27(±9)
M68-3	153	0.6(±0.1)	14(±4)
P399-2	341	1.1(±0.3)	25(±8)
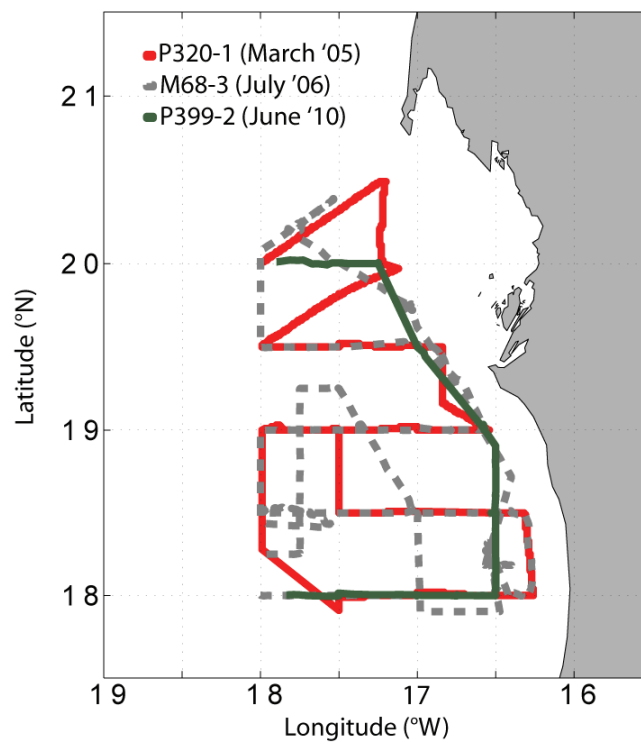
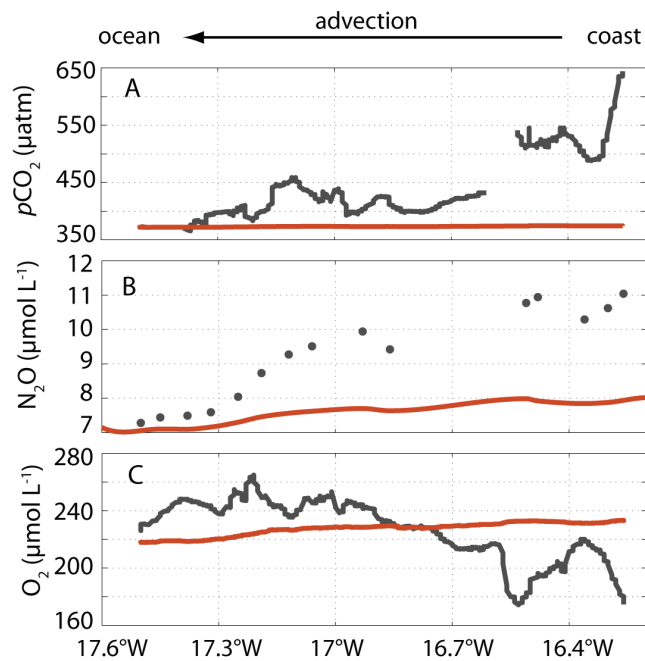**Fig. 1.** Location of the cruise tracks of the three cruises used in this study.

Fig. 2. Underway measurements during P320-1 (March 2005) along the 18° N transect. Black lines/markers denote measured values in surface seawater, red lines denote atmospheric values for CO_2 **(A)** and saturation concentration for N_2O **(B)** and O_2 **(C)**, both calculated from temperature and salinity. The coastal upwelling is characterized by high supersaturation of CO_2 and N_2O and undersaturation of O_2.
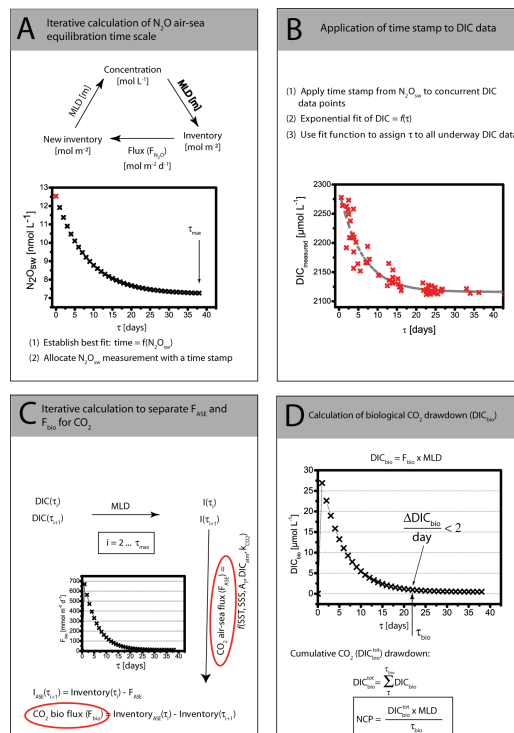
Fig. 3. Calculation scheme to obtain NCP. The red marked values are measured data, the black ones were calculated. For details please refer to text. The shown data are taken from cruise P320-1.
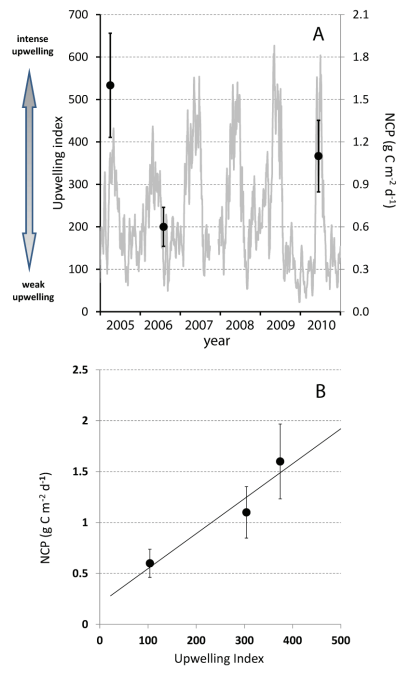
Fig. 4. (A) Seasonality of the Mauritanian upwelling as illustrated by the upwelling index (grey line) and NCP values estimated in this study. **(B)** Relationship between NCP and upwelling index. The black line represents a linear regression.

4875